Efficient model for the prediction of dendritic grain growth using the lattice Boltzmann method coupled with a cellular automaton algorithm

IOP Conf. Series: Materials Science and Engineering **529** (2019) 012028 doi:10.1088/1757-899X/529/1/012028

Efficient model for the prediction of dendritic grain growth using the lattice Boltzmann method coupled with a cellular automaton algorithm

Stephan Jäger[1] and Andreas Ludwig[2]

[1] Light Metals Technologies Ranshofen, Center for Low-Emission Transport, Austrian Institute of Technology, 5282 Braunau am Inn - Ranshofen, Austria
[2] Simulation and Modelling of Metallurgical Processes, Department of Metallurgy, University of Leoben, 8700 Leoben, Austria

E-mail: stephan.jaeger@ait.ac.at

Abstract. An efficient model for the prediction of dendritic grain growth is developed coupling the lattice Boltzmann method for solving the transport of solute and a cellular automaton algorithm for determining the evolution of grains' envelope and the release of solute during phase change. In contrast to solving equations from the field of continuum mechanics the new model is more related to particular occasions what is more similar to the behaviour of cellular automaton algorithms. The resulting dendritic grain growth shows qualitative correctness, although the consideration of solute conservation is still missing. It is shown that neglecting proposed conditions regarding the choice of time step size can destabilize the solid-liquid interface resulting in secondary and ternary dendrite arms.

1. Introduction

There are several approaches of simulating dendritic grain growth. Besides phase field and front tracking simulations, cellular automaton (CA) is quite often used based on the work presented by Gandin and Rappaz [1, 2]. Herein, the evolution of the grain's envelope is related to the thermal undercooling using the model proposed by Kurz, Giovanola and Trivedi (KGT)[3, 4] for rapid solidification. This approach is extended in [5] considering solute and curvature undercooling and continued for three dimensions [6]. It is coupled to the lattice Boltzmann method (LBM) considering fluid flow in [7, 8] and compared with results from phase field simulations in [9]. A different approach is chosen in [10] employing thermal LBM with an enthalpy-porosity technique for the simulation of dendritic grains with fluid flow. These all have in common the calculation of the curvature of the interface between the solid and liquid phase what is demanding on the resolution and the computational effort calculating spatial gradients.

The objective of the present work is to more efficiently simulate solidification offering dendritic structures using a CA for determining the evolution of growing grains and the LBM for solving transport of solute. The proposed model aims to be more accurate with respect to the grain shape and microsegregation than the original CA of [1, 2] by considering solutal undercooling. In contrast to [11, 7, 10] undercooling due to the curvature of the solid-liquid interface is neglected. Thus, no gradients using the finite difference method have to be computed. The new approach should not act as an alternative for solving continuum mechanical equations in

its equilibrium state but combining the state driven behaviour of cellular automaton [12] and analytical equations. The increased efficiency should enable the integration of grain growth models in full scale industrial application in the future.

2. Model description

LBM is coupled with a CA for the simulation of the dendritic grain growth. These are not weakly but fully coupled following the categorization of [13]. Compared to previously mentioned work the release of solute is not done in the way of continuum mechanics but following the idea of discrete occasions which is explained at the end of this section.

2.1. Lattice Boltzmann method for solute transport

LBM is applied for the computation of the diffusion of solute c neglecting any advection

$$\frac{\partial c}{\partial t} = D\frac{\partial^2 c}{\partial x^2} \tag{1}$$

assuming constant diffusivity D. LBM is based on the relaxation of non-equilibrium states derived from a statistical distribution of particles. There are basically two operatrions which define the computational sequence: there are the *collision* and the *streaming* operation. The *collision* of the discrete distribution of particles $g_i(\vec{x}, t+1)$ at the spatial position $\vec{x}$ and the time $t+1$ is determined as

$$g_i(\vec{x}, t+1) = g_i(\vec{x}, t) - \frac{1}{\tau}(g_i(\vec{x}, t) - g_i^{eq}(\vec{x}, t)). \tag{2}$$

using the Bathnagar-Gross-Krook dynamics with its linear collision operator [14, 15] and the relaxation time τ. The equilibrium state $g_i^{eq} = cw_i$ is defined using the lattice weights w_i following the multiscale Chapman-Enskog analysis [16]. The solute is reconstructed by

$$c = \sum_{i=0}^{n-1} g_i. \tag{3}$$

The sum is limited by the amount n of discrete velocities $\vec{e_i}$ and corresponding weights w_i which depend on the chosen lattice. On the two-dimensional cartesian grid, the D2Q5 lattice with $n = 5$ is chosen. This reduces the computational effort and the requirements regarding memory capacity compared to the commonly used D2Q9 lattice. The D2Q5 lattice guarantees second order rotational invariance [16]. This is sufficient for the reconstruction of a diffusion equation. The diffusivity D in equation 1) is related to the relaxation time τ by

$$D = c_s^2(\tau - \frac{1}{2})\frac{\Delta x^2}{\Delta t} \tag{4}$$

with the lattice speed of sound $c_s = 1/\sqrt{3}$ for the D2Q5 lattice. Δx and Δt are the spatial and the temporal discretizations which have to be chosen in a way that $\tau > 1/2$. Thus, the relaxation time τ is defined for the liquid and the solid phase depending on the diffusivity in the liquid D_l and in the solid phase D_s, respectively.

The *collision* is fully local which requires no communication to neighbouring voxels (discretization points) since the left hand side and the right hand side of equation 2 are function of $\vec{x}$. Whereas, the *streaming* operation streams information from $\vec{x}$ to the next neighbour $\vec{x}+\vec{e_i}$ which is defined as

$$g_i(\vec{x} + \vec{e_i}, t+1) = g_i(\vec{x}, t+1). \tag{5}$$

2.2. Grain growth algorithm

The CA algorithm for simulating the evolution of growing grains is derived from the original work [1, 2] and the decentred squares [17]. The state of a cell - it can be either liquid, interface or solid - and its evolution depend on the state of the neighbouring cells, the local temperature and the local solute. Thus, it is not fully local because there are eight neighbours (and the cell itself) in two dimensions using a cartesian grid. In the original CA grain growth algorithm, the spatial discretization Δx is recommended to be about the secondary dendrite arm spacing λ_2 [2]. For the binary alloy Al-Cu and moderate cooling rates, the secondary dendrite arm spacing is estimated to $\lambda_2 \approx 10 - 40$ µm [18] for a parameter study. In the modified CA algorithms the spatial resolution has to be much smaller since the models fully resolve the interface and the secondary dendrite arms as well. For this, the spatial resolution is chosen $\Delta x \approx 1$ µm or even smaller [11, 7, 9]. In the presented model, the spatial discretization should be 1 µm $< \Delta x < \lambda_2$ to become more reliable for large-scale applications with respect to the computational effort. Since the discretization can be chosen in a way the secondary dendrite arms can not be resolved, different models have to be applied. Therefore, the grain growth algorithm is defined for two regions. The inner region Ω_{in} is enclosed by the envelope region Ω_{env}. The envelope region Ω_{env} describes the interface between the fully liquid and the partially solid region with the solid fraction $0 < f_s \ll 1$ whereas Ω_{in} can be fully solid or partially solid ($0 < f_s \leq 1$). Basically, the models are taken from the work presented in [19] and adapted in a way to get more precise information about the grain shape. In all cases the growth velocity is related to the supersaturation

$$\Omega = \frac{c_l^* - c_l}{c_l^* - c_s^*} = \frac{c_l^* - c_l}{c_l^*(1-k)} \tag{6}$$

with the partition coefficient $k = c_s^*/c_l^*$, solid c_s^* and liquid c_l^* solutal equilibrium concentration and local liquid concentration c_l. It is assumed that for Ω_{env} the model proposed by Lipton, Glicksman and Kurz (LGK) [20, 4] is valid although it is derived assuming a paraboloid primary dendrite tip in steady state condition without any neighbours. The growth velocity v_{env} is determined as [20]

$$v_{env} = v_{tip} = v_{LGK} = \frac{D_l \; m_l \; c_l(k-1)}{\Gamma \pi^2} (Iv^{-1}(\Omega))^2 \tag{7}$$

with the solute diffusivity D_l, the liquidus slope m_l, the solute concentration of the liquid c_l, Gibbs-Thomson coefficient Γ and the inverse of the Ivantsov equation $Iv^{-1}(\Omega)$ for the two-dimensional space [21]. The initialization of the solid fraction for the inner region $f_{s,init}$ after going through the envelope region Ω_{env} has to be assumed at the current state of this work. For the inner region, the growth velocity is defined as

$$v_{in} = \frac{D_l}{l_d} \frac{c_l^* - c_l}{c_l^*(1-k)} \tag{8}$$

substituting the interdendritic (liquid) concentration c_d from [19] by the liquid concentration c_l. The characteristic diffusion length l_d can be estimated according to [22] by $l_d = \beta_2(\lambda_2 - d_2)/2$ with the diameter of the secondary dendrite arm d_2, and the constant $\beta_2 = 1.0$. It can be approximated by [19]

$$l_d = \beta_2 \frac{\lambda_2 f_l}{2}. \tag{9}$$

substituting the interdendritic liquid f_d^e in [19] by the local liquid fraction f_l within Ω_{in}. The equation for the growth algorithm is applied as long as the the cell is still partially liquid $f_s < 1$. If $f_s = f_{s,limit}$ the cell becomes fully solid and the diffusivity is changed to $D = D_s$. A surface area concentration S is missing in combination with the growth velocity v_{in} for determining the change of the solid fraction $df_s/dt = v_{in}\ S$. The envelope liquid fraction f_e is substituted by

the liquid fraction f_l and the Avrami factor in [19] is neglected due to the increased resolution compared to [19]. This results in the surface area concentration

$$S = \frac{2}{\lambda_2} f_l. \tag{10}$$

Following this approach, results in a non-discrete interface between the liquid and the solid region and the co-existence of solid solute and liquid solute at each cell are allowed. It is an averaged field of solute and solid fraction. Thus, if one would determine the solute only depending on the solid fraction [7] the solute at the envelope region would be underestimated and the high gradients, especially close to the primary dendrite tip, would not be represented. This would lead to an underestimated concentration field and a wrong tip velocity using the LGK model. Therefore, the solute release is defined as a particular occasion setting the concentration of the liquid phase $c_l = c_l^*$ and the concentration for the solid phase $c_s = c_s^*$. These are defined each time the integrated growth velocity over time t

$$l = \int_{t_{j-1}}^{t_j} v \; dt \tag{11}$$

exceeds a certain characteristic length l starting at the last time an occasion occured t_{j-1} until the current time t_j. The characteristic length is determined as the spatial resolution $l = \Delta x$. The growth velocity v is either the one of the envelope region v_{env} or the inner region v_{in}. Subsequently, the released solute is diffused in the liquid phase using LBM. The time step for the simulation basically depends on several parameters. Thus, it is restricted by the stability of LBM for the transport of solute (see eq. 4) and by the growth velocity of CA. The supersaturation can restrict the time step for the CA depending on the cooling rate. The time step is defined depending on the maximum of velocity v_{env} with the scale factor γ - which is in general bounded by $0 < \gamma \leq 1$ for a stable algorithm and proposed to be chosen as $\gamma = 1/10$ in [23]:

$$\Delta t = \gamma \, \frac{\Delta x}{\max\{v_{env}(c_l)\}}. \tag{12}$$

3. Simulation setup

The evolution of a single equiaxed grain with the crystallographic orientation of 20° in an Al-4.7wt.%Cu alloy is simulated in a two-dimensional domain of the size 1 mm x 1 mm. The alloy related parameters are listed in table 1 taken from [18]. The simulation starts at the liquidus temperature T_l and is isotropically reduced applying a constant cooling rate $\dot{T} = 30$ K/s. The free model parameters λ_2, $f_{s,init}$ and $f_{s,limit}$ are assumed to be constant (see table 1). Two spatial resolutions are distinguished: (1) $\Delta x = 5$ µm and (2) $\Delta x = 2.5$ µm. The time step is defined equally for both spatial resolutions as $\Delta t = 1.5 \cdot 10^{-4}$ s. Thus, for the higher resolved simulation $\gamma \leq 1$ is not fulfilled (see eq. 12) which results in a destabilized behaviour.

Table 1 Simulation parameters for Al-4.7wt.%Cu

Thermophysical properties	Thermodynamic properties	Model parameters
$D_l = 3 \cdot 10^{-9}$ m^2/s	$T_m = 933.5$ K	$\lambda_2 = 10$ µm
$D_s = 8 \cdot 10^{-13}$ m^2/s	$m_l = -344$ K	$f_{s,init} = 0.1$
$L = 3.97 \cdot 10^5$ J/kg	$k = 0.145$	$f_{s,limit} = 0.85$
$\rho_s \approx \rho_l = 2743$ kg/m^3	$\Gamma = 2.41 \cdot 10^{-7}$ m K	

4. Results

At time $t = 0.87$ s and $t = 1.02$ s the extent of the dendrite tips and the solute concentration is different with respect to the spatial resolution (see figure 1). Herein, the solute concentration is determined as $c = c_l(1 - f_s) + c_s f_s$. Focusing on the solid fraction f_s, the lower resolution (left half of the pictures) shows a more averaged field whereas the higher resolution (right half of the pictures) shows some detailed resolved secondary dendrite arms ($f_s > 0$). The solute concentration at $t = 1.02$ s shows a characteristic behaviour of this algorithm: resolution (1) with the stable CA shows a very diffusive behaviour. In contrast, resolution (2) with the unstable CA shows less dominant diffusion. There is a very high gradient of the solute concentration close to the liquid-solid interface especially in the region of secondary dendrite tips which seem to overtake the diffusive process. Further refining as well as coarsening shows that the results are strongly dependent on the spatial resolution. In general the solute is not conserved using this approach. The change of solute over time depends on the growth velocity and in most cases the total solute strongly increases.

The destabilized simulation shows secondary dendrite arms and even tertiary dendrite arms in a later stage. It seems to be physical in a way, but the destabilization is not related to the interface anisotropy. In the present work it is related to the ratio of user-defined time step and growth velocity which again depend on the solute and thermal undercooling.

The simulation time for the stable and the destabilized setup is 25 s and 96 s, respectivley, running in parallel on a quadcore notebook processor.

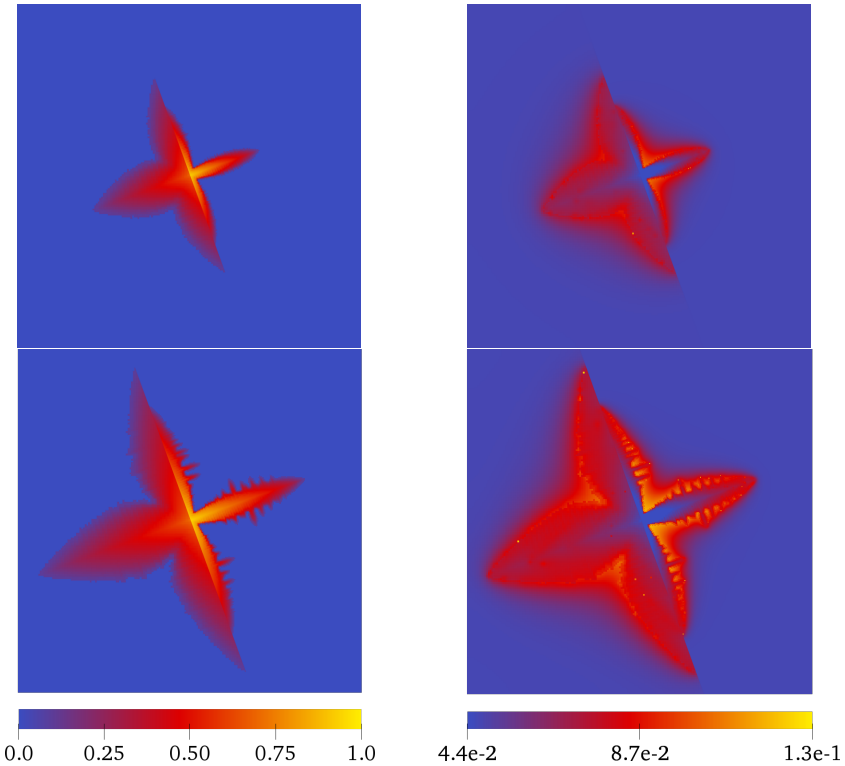

(a) Solid fraction f_s (b) Solute concentration c

Figure 1 Solid fraction f_s and solute concentration c during equiaxed dendritic solidification with the crystallographic orientation of 20° in an isotropically undercooled ($\dot{T} = 30$ K/s) Al-4.7wt.%Cu melt at two different times $t = 0.87$ s (top) and $t = 1.02$ s (bottom) for resolution (1) (left half in each figure) and resolution (2) (right half)

5. Discussion

The presented model meets the expecations regarding the determination of grain growth showing secondary dendrite arms or an averaged field depending on the user-defined resolution. On the contrary, the solute is not conserved and the accuracy depends on the spatial and temporal resolution. This also related to the issue that there is no energy or force at the envelope which pushes the solute concentration which has to be improved in future work. There is no sharp transition of phases. Future modification has to strongly focus on the conservation of species.

Furthermore, it has been shown that growing secondary dendrite arms can be simulated using a destabilized simulation setup. For physically correct destabilzation the condition regarding the growth veocity and the influence of spatial and temporal resolution has to be further investigated.

6. Outlook

This work should constitute the basis for more sophisticated simulations considering the interaction of multiple grains, microsegregation as well as the transport of grains in 3D. Therefore, the future work will heavily focus on the efficiency of the newly developed model considering the conservation of species. Furthermore, its application in the three-dimensional space must be approved.

Acknowledgments

The Author would like to thank the Austrian Research Promotion Agency (FFG), the Federal Ministry for Transport, Innovation and Technology (BMVIT) and the State of Upper Austria for funding this work. This work was conducted in the framework of COMET project Amoree (Grant: 843537) and the framework of FTI Struktur Land Oberösterreich of Upper Austria project PSHeRo.

References

[1] Rappaz M and Gandin C A 1993 *Acta Metallurgica et Materialia* **41** 345–360
[2] Gandin C A and Rappaz M 1994 *Acta Metallurgica et Materialia* **42** 2233–2246
[3] Kurz W, Giovanola B and Trivedi R 1986 *Acta Metallurgica* **34** 823 – 830
[4] Kurz W and Fisher D 1986 *Fundamentals of solidification* Bd. 1 (Trans Tech Publications)
[5] Zhu M F and Hong C P 2001 *ISIJ International* **41** 436–445
[6] Zhu M F and Hong C P 2002 *ISIJ International* **42** 520–526
[7] Sun D, Zhu M, Pan S and Raabe D 2009 *Acta Materialia* **57** 1755 – 1767
[8] Sun D, Zhu M, Wang J and Sun B 2016 *International Journal of Heat and Mass Transfer* **94** 474–487
[9] Zaeem M A, Yin H and Felicelli S D 2013 *Applied Mathematical Modelling* **37** 3495 – 3503
[10] Chatterjee D and Chakraborty S 2006 *Physics Letters A* **351** 359–367
[11] Luo S and Zhu M Y 2013 *Computational Materials Science* **71** 10 – 18
[12] Chopard B and Droz M 1998 *Cellular Automata Modeling of Physical Systems* Collection Alea-Saclay: Monographs and Texts in Statistical Physics (Cambridge University Press)
[13] Gandin C A, Desbiolles J L, Rappaz M and Thevoz P 1999 *Metallurgical and Materials Transactions A* **30** 3153–3165
[14] Qian Y H, D'Humières D and Lallemand P 1992 *EPL (Europhysics Letters)* **17** 479
[15] Lallemand P and Luo L S 2000 *ICASE Report* 1–33
[16] Latt J 2007 *Hydrodynamic Limit of Lattice Boltzmann Equations* Ph.D. thesis University of Geneva
[17] Gandin C A and Rappaz M 1997 *Acta Materialia* **45** 2187–2195
[18] Wu M and Ludwig A 2009 *Acta Materialia* **57** 5632 – 5644
[19] Wu M and Ludwig A 2009 *Acta Materialia* **57** 5621 – 5631
[20] Lipton J, Glicksman M and Kurz W 1984 *Materials Science and Engineering* **65** 57 – 63
[21] Dantzig J and Rappaz M 2016 *Solidification: 2nd Edition* Engineering Sciences (EPFL Press)
[22] Wang C Y and Beckermann C 1993 *Metallurgical and Materials Transactions A* **24** 2787–2802
[23] Rai A, Markl M and Körner C 2016 *Computational Materials Science* **124** 37–48